# Research

# Monitoring Intracellular Redox Changes in Ozone-Exposed Airway Epithelial Cells

*Eugene A. Gibbs-Flournoy,[1] Steven O. Simmons,[2] Philip A. Bromberg,[3] Tobias P. Dick,[4] and James M. Samet[5]*

[1]Curriculum in Toxicology, University of North Carolina at Chapel Hill, Chapel Hill, North Carolina, USA; [2]Integrated Systems Toxicology Division, National Health and Environmental Effects Research Laboratory (NHEERL), U.S. Environmental Protection Agency (EPA), Research Triangle Park, North Carolina, USA; [3]Center for Environmental Medicine, Asthma and Lung Biology, University of North Carolina at Chapel Hill, Chapel Hill, North Carolina, USA; [4]Division of Redox Regulation, DKFZ-ZMBH Alliance, German Cancer Research Center (DKFZ), Heidelberg, Germany; [5]Environmental Public Health Division, NHEERL, U.S. EPA, Chapel Hill, North Carolina, USA

**BACKGROUND:** The toxicity of many xenobiotic compounds is believed to involve oxidative injury to cells. Direct assessment of mechanistic events involved in xenobiotic-induced oxidative stress is not easily achievable. Development of genetically encoded probes designed for monitoring intracellular redox changes represents a methodological advance with potential applications in toxicological studies.

**OBJECTIVE:** We tested the utility of redox-sensitive green fluorescent protein (roGFP)–based redox sensors for monitoring real-time intracellular redox changes induced by xenobiotics in toxicological studies.

**METHODS:** roGFP2, a reporter of the glutathione redox potential ($E_{GSH}$), was used to monitor $E_{GSH}$ in cultured human airway epithelial cells (BEAS-2B cells) undergoing exposure to 0.15–1.0 ppm ozone ($O_3$). Cells were imaged in real time using a custom-built $O_3$ exposure system coupled to a confocal microscope.

**RESULTS:** $O_3$ exposure induced a dose- and time-dependent increase of the cytosolic $E_{GSH}$. Additional experiments confirmed that roGFP2 is not directly oxidized, but properly equilibrates with the glutathione redox couple: Inhibition of endogenous glutaredoxin 1 (Grx1) disrupted roGFP2 responses to $O_3$, and a Grx1-roGFP2 fusion protein responded more rapidly to $O_3$ exposure. Selenite-induced up-regulation of GPx (glutathione peroxidase) expression–enhanced roGFP2 responsiveness to $O_3$, suggesting that (hydro)peroxides are intermediates linking $O_3$ exposure to glutathione oxidation.

**CONCLUSION:** Exposure to $O_3$ induces a profound increase in the cytosolic $E_{GSH}$ of airway epithelial cells that is indicative of an oxidant-dependent impairment of glutathione redox homeostasis. These studies demonstrate the utility of using genetically encoded redox reporters in making reliable assessments of cells undergoing exposure to xenobiotics with strong oxidizing properties.

**KEY WORDS:** glutathione, human airway epithelial cells, imaging, intracellular, oxidative stress, ozone, NADPH, redox, roGFP. *Environ Health Perspect* 121:312–317 (2013). http://dx.doi.org/10.1289/ehp.1206039 [Online 18 December 2012]

The intracellular redox environment is a highly dynamic setting governed by the formation and degradation of various reactive species of oxygen and nitrogen. Under normal physiological conditions, the cytosol, the nucleus, and the mitochondrial matrix space maintain homeostatic conditions in favor of a highly reducing environment (Cannon and Remington 2008). Intracellular reducing conditions are largely maintained by millimolar concentrations of reduced glutathione and its accessory enzymes that together constitute the glutathione system (Anderson 1998). Ultimately, maintenance of the intracellular glutathione redox potential ($E_{GSH}$) comes from the metabolism of glucose because glutathione is reduced by glutathione reductase using NADPH (nicotinamide adenine dinucleotide phosphate) produced by the pentose phosphate pathway (PPP) (Wamelink et al. 2008).

A number of pathophysiological states are associated with changes in the $E_{GSH}$ (Dubinina and Dadali 2010; Ma 2010; Yang and Omaye 2009). Such "oxidative stress" is commonly cited as a mechanistic feature of the toxicity of numerous xenobiotic compounds linked to adverse health outcomes (Bargagli et al. 2009; Ciencewicki et al. 2008; Kohen and Nyska 2002). For instance, the health effects of the potent ambient air pollutant ozone ($O_3$) are understood to be mediated through an oxidative stress mechanism involving the oxidation of cellular biomolecules (Ballatori et al. 2009; Kelly et al. 1995; Mudway and Kelly 2000). In the lung, $O_3$ exposure causes decrements in pulmonary function and induces inflammatory responses derived from the bronchial epithelium, a major target of $O_3$ exposure (Ballinger et al. 2005; Ciencewicki et al. 2008; Kelly et al. 1995; Mudway and Kelly 2000; Pryor 1992; Pryor et al. 1995; Song et al. 2010). Because of its high reactivity, $O_3$ interacts with cellular and extracellular biomolecules, resulting in multiple types of oxidative damage to lipids, proteins, and nucleic acids (Kelly et al. 1995; Laumbach 2010; Mudway and Kelly 2000; Srebot et al. 2009; van der Vliet et al. 1995; Yang and Omaye 2009). While numerous studies have established oxidant damage of biomolecules as a result of $O_3$ exposure, direct measures of $O_3$-mediated "oxidative stress" have been difficult to achieve; yet alteration of a defined intracellular redox couple like the glutathione redox pair (GSH/GSSG) would represent an important early indicator of the oxidative effects of $O_3$ exposure.

Recent methodological advances have made it possible to focus studies of prooxidative changes to specific redox couples within defined subcellular compartments (Meyer and Dick 2010), potentially affording greater specificity in mechanistic investigations of the oxidative effects of xenobiotic exposures. A new generation of genetically encoded fluorophores permits direct assessment of the oxidative effects of xenobiotic compounds in relation to the GSH/GSSG redox pair with unprecedented spatial and temporal resolution (Cheng et al. 2012; Dooley et al. 2004; Meyer and Dick 2010). Redox-sensitive green fluorescent protein 2 (roGFP2) acts as a reporter of intracellular $E_{GSH}$ by equilibrating with the GSH/GSSG redox pair (Gutscher et al. 2008; Meyer and Dick 2010; Morgan et al. 2011). In short, in a reaction that depends on catalysis by glutaredoxins, roGFP2 responds to oxidation of reduced glutathione (GSH) to its oxidized form (GSSG) via the internal formation of a disulfide bond (Gutscher et al. 2008; Meyer 2008; Meyer and Dick 2010) (Figure 1). The formation of the disulfide bond alters the spectral characteristics of the GFP fluorophore causing the intensity of the emitted green fluorescence (~ 520 nm) induced by excitation at 488 nm to decrease, while causing the emitted fluorescence after excitation at 405 nm to increase, thus making this sensor a ratiometric

probe. Further efforts to improve the responsiveness of roGFP2 have led to the conjugation of pathway-specific enzymes to create a chimeric fusion of proteins operating as redox relays. In particular, the conjugation of glutaredoxin 1 (Grx1) to roGFP2 has been shown to enhance the kinetics of the roGFP2 response to the oxidation of glutathione (Gutscher et al. 2008).

In the present study, we used live-cell microscopy to monitor the cytosolic $E_{GSH}$ of airway epithelial cells undergoing exposure to $O_3$ in real time. Here, we report an approach to validate the use of roGFP2-based redox sensors in toxicological studies of xenobiotics with strong oxidizing properties.

## Methods

*Materials and reagents.* We purchased tissue culture media and supplements from Lonza (Walkersville, MD, USA), and Wilco Wells glass-bottom culture dishes from Ted Pella Inc. (Redding, CA, USA) and Warner Instruments (Hamden, CT, USA). Fugene 6 transfection reagent was acquired from Roche Applied Science (Indianapolis, IN, USA). Kits to measure intracellular glutathione and NADPH were bought from Promega (Madison, WI, USA) and AbCam (Cambridge, MA, USA), respectively. Laboratory reagents and chemicals including hydrogen peroxide ($H_2O_2$), dithiothreitol (DTT), 2-acetylamino-3-[4-(2-acetylamino-2-carboxyethylsulfanylthiocarbonylamino)phenylthiocarbamoylsulfanyl] propionic acid (2-AAPA), buthionine sulfoximine (BSO), and sodium selenite were obtained from Sigma-Aldrich (St. Louis, MO, USA). Basic laboratory supplies were purchased from Fisher Scientific (Raleigh, NC, USA).

*Cell culture.* Transformed human airway epithelial cells [BEAS-2B, subclone S6 (Reddel et al. 1988)] were cultured as previously described (Tal et al. 2010) and maintained in serum-free keratinocyte growth medium (KGM; Lonza). The cells were incubated in a humidified incubator at 37°C in 5% carbon dioxide ($CO_2$). For most live-cell exposures, BEAS-2B cells were plated in 35 mm Wilco Wells glass-bottom dishes with a 12 mm #1.5 glass aperture (Ted Pella Inc.).

*Genetically encoded redox sensors.* Plasmid for roGFP2 was the generous gift of S.J. Remington (University of Oregon, Eugene, OR, USA). Plasmid for the $H_2O_2$ sensor, HyPer, was purchased from Evrogen (Axxora, Farmingdale, NY, USA). Cytosolic and mitochondrially targeted versions of roGFP2 and HyPer were placed into lentiviral vectors as described previously (Cheng et al. 2012).

*Plasmid transfection and lentiviral transduction.* One to 2 days before exposure, BEAS-2B cells were transiently transfected with 1–2 µg of plasmid DNA encoding Grx1-roGFP2, HyPer, or roGFP2 using 3–5 µL of Fugene 6 transfection reagent for

each 35 mm culture dish. Stable expression of a specific genetically encoded fluorescent reporter was performed via lentiviral transduction. In short, a lentivirus encoding roGFP2 or HyPer (i.e., specifically targeted to the cytosol or mitochondria, respectively) was incubated for 4 hr (at 37°C in 5% $CO_2$) with wild-type BEAS-2B cells using a multiplicity of infection of 5–10 in a single well of a 6-well dish. The viral particles were then removed and fresh KGM was placed on the cells, and the BEAS-2B cells were then allowed to grow to confluency. Upon confluency, the cells were expanded to T75 dishes where they were propagated for multiple passages. For some experiments, stably transduced cells were sorted for optimal fluorescence expression at the University of North Carolina at Chapel Hill Core Flow Cytometry Facility.

*Exposure conditions.* Newly transfected or stably transduced BEAS-2B cells expressing the fluorescent reporter of interest were cultured as described above. Prior to exposure, subconfluent cells were equilibrated in Locke solution (Taylor-Clark and Undem 2010) for 2 hr at 37°C in 5% $CO_2$. For the studies herein, two versions of Locke solution were derived by adding (LS + G) or excluding (LS − G) 1 mg/mL DL-glucose. Irrespective of the type of Locke solution used to equilibrate cells, all live-cell $O_3$ exposures were performed using 0.5 mL of LS − G. For all imaging experiments, cells were exposed in a custom-built stage-top exposure system maintained at 37°C with 1.5 L/min of 5% $CO_2$/balance air at a relative humidity of ≥ 95% [see Supplemental Material, Figure S1

(http://dx.doi.org/10.1289/ehp.1206039)]. In some experiments, cells were pretreated with 100 µM 2-AAPA, a dithiocarbamate inhibitor of glutaredoxins, during the 2-hr buffer equilibration period. Similarly, pretreatment of cells with 1 µM sodium selenite for 24–48 hr before $O_3$ exposure was carried out to induce the overexpression of glutathione peroxidases (GPx).

For each experiment, cells were exposed to control air (5% $CO_2$/balance air) or to $O_3$ concentrations ranging from 0.15–1.0 ppm. The entire exposure period typically consisted of three component intervals collectively lasting ≤ 1 hr. They included *a*) an initial untreated baseline period of 5 min; *b*) an exposure period of ≤ 45 min; and *c*) a 10-min control exposure period in which cells were oxidized by 0.1–1.0 mM $H_2O_2$ for 5 min and then reduced by 10 mM DTT for an additional 5 min. During these exposures, the $O_3$ concentration in the exposure chamber was monitored in real time using a Dasibi model 1003-AH $O_3$ analyzer (Dasibi Environmental Corporation, Glendale, CA, USA) sampling at a flow of 2.0 L/min. $O_3$ exposures for non-imaging assays were performed using exposure chambers operated by the U.S. Environmental Protection Agency's Environmental Public Health Division.

*Imaging analysis.* All live-cell experiments done in real time were conducted using a Nikon Eclipse C1si spectral confocal imaging system equipped with an Eclipse Ti microscope, Perfect Focus System, and 404 nm, 488 nm, 561 nm, and 633 nm primary laser lines (Nikon Instruments Corporation,
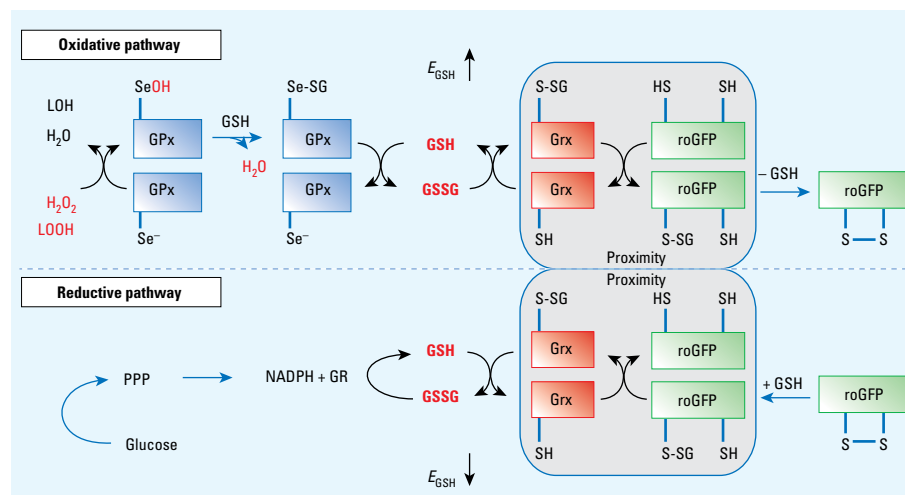


**Figure 1.** roGFP2 interactions with the glutathione system (adapted from Meyer and Dick 2010). Glutathione peroxidases (GPx) oxidize GSH to GSSG in response to peroxides, including $H_2O_2$ and lipid hydroperoxides (LOOHs), thus increasing the glutathione redox potential ($E_{GSH}$). Abbreviations: LOH, reduced lipid oxide; Se⁻, reduced selenocyteine; SeOH, oxidized selenocyteine; SeSG, glutathionylated selenocysteine. In response to the increase in GSSG, one of the engineered vicinal cysteines of roGFP2 becomes *S*-glutathionylated by glutaredoxin (Grx). Glutathionylation in turn causes disulfide bond formation and alteration of the spectral properties of the GFP fluorophore. In the reductive pathway, Grx catalyzes the reduction of roGFP2 disulfide bonds through deglutathionylation as GSSG levels decrease and normal levels of GSH are reestablished by glutathione reductase (GR), at the expense of NADPH, causing a renormalization of $E_{GSH}$. Glucose and the pentose-phosphate pathway (PPP) create NADPH, which is used by GR to reduce GSSG to GSH.

Melville, NY, USA). Images were acquired using a 60× Plan Apo lens. For experiments involving the genetically encoded fluorescent reporters, roGFP2 and HyPer, green fluorescence was observed via the use of independent excitations at 404 and 488 nm, and emitted light was collected for each using a 525/30 nm band-pass filter (Chroma, Bellows Falls, VT, USA). Results were calculated as ratios of the emissions excited by the 488 nm and 404 nm lasers scanned sequentially at a frequency of 1 min. All imaging data were acquired using Nikon EZ-C1 software.

*Measurement of intracellular NADPH.* After cells were equilibrated in fresh KGM or Locke solution (LS + G or LS – G) for 2 hr, the intracellular levels of total NADPH were assessed using an AbCam (Cambridge, MA, USA) NADP/NADPH assay kit according to the manufacturer's instructions. Following the equilibration period, cells were immediately placed on ice and washed with cold 1× PBS just before the initial lysis step. Absorbance was read at 450 nm using a PolarStar Optima microplate reader (BMG Labtech, Durham, NC, USA).

*Statistical analysis.* All imaging data were quantified using NIS-Elements AR software (Nikon). For each experiment, the responses of 5–10 cells were collected as regions of interest and then averaged to derive an overall response. Data are expressed as the mean of at least three repeated experiments. Pairwise comparisons of control and treatment groups were performed using analysis of variance and linear regression, with $p < 0.05$ as statistically significant.
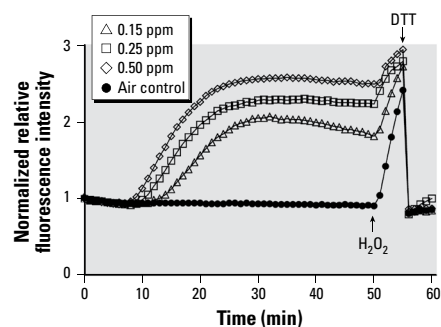


**Figure 2.** Exposure to $O_3$ induces a dose- and time-dependent increase in the cytosolic $E_{GSH}$ in airway epithelial cells. BEAS-2B cells expressing cytosolic roGFP2 were exposed to clean air for 5 min followed by a 0 (air control), 0.15, 0.25, or 0.50 ppm $O_3$ exposure for 35 min in a stage-top exposure system maintained at 37°C, > 90% relative humidity, and 5% $CO_2$. Shown are ratiometric values (404/488) calculated from the fluorescence intensity emitted at 510 nm induced by sequential excitation at 404 and 488 nm, plotted relative to the 5-min baseline. Addition of 0.1 mM $H_2O_2$ at the end of the $O_3$ exposure produced a maximal response, which was fully reversible with the addition of 10 mM DTT. The data shown were derived from three or more separate experiments monitoring seven or more cells in real time throughout the exposure period.

# Results

*$O_3$ exposure induces an increase in the cytosolic $E_{GSH}$.* The presence of glucose in the exposure media is known to shorten the half-life of $O_3$ (Taylor-Clark and Undem 2010). Therefore, in these experiments, cells were first equilibrated in LS + G for 2 hr, and then switched to LS – G for the exposure. Exposure of BEAS-2B cells expressing cytosolic roGFP2 to 0.15–0.50 ppm $O_3$ resulted in a dose- and time-dependent probe response, reflecting an increase in the cytosolic $E_{GSH}$ [Figure 2; see also Supplemental Material, Figure S5 (http://dx.doi.org/10.1289/ehp.1206039)]. Increasing $O_3$ concentration hastened the onset while elevating the magnitude of the oxidative response reported by roGFP2 (Figure 2). Adding 0.1 mM $H_2O_2$ at the end of each $O_3$ exposure produced a maximal response, which was fully reversible with the addition of 10 mM DTT.

*Glucose deprivation potentiates the elevation of $E_{GSH}$ induced by $O_3$ exposure.* On an individual basis, BEAS-2B cells equilibrated in the presence of glucose (i.e., in LS + G) were observed to respond variably to a given concentration of $O_3$, suggesting substantial heterogeneity of redox homeostasis within the cellular population under the given conditions. Figure 3A shows the individual responses of seven BEAS-2B cells in the same field of view being exposed to 0.5 ppm $O_3$, with some cells responding with strongly increasing $E_{GSH}$, while others responded only minimally. Furthermore, some cells exhibited an intermediate response followed by a recovery of $E_{GSH}$ despite continued $O_3$ exposure. Given the importance of PPP-generated NADPH in maintaining intracellular GSH levels, we hypothesized that glucose deprivation would sensitize the cells to a subsequent $O_3$ exposure. As shown in Figure 3B, depriving the cells of glucose for 2 hr before exposure homogenized the magnitude, time of onset, and rate of response of the cells to $O_3$. Glucose status did not affect the probe response to the addition of $H_2O_2$ and DTT

(Figure 3A,B). As expected, glucose deprivation led to decreased cellular NADPH levels [see Supplemental Material, Figure S2 (http://dx.doi.org/10.1289/ehp.1206039)].

*Validation of glutathione-dependent roGFP2 responses to $O_3$ exposure.* Given the extreme reactivity of $O_3$ with biomolecules, we considered the possibility that the spectral changes of the probe interpreted as changes in $E_{GSH}$ are the result of a direct oxidation of roGFP2 by $O_3$ itself or by an $O_3$-generated secondary oxidant. We therefore undertook a series of experiments to determine whether $O_3$-induced changes in the roGFP2 fluorescence intensity ratio involve components of the glutathione system through which roGFP2 has been demonstrated to respond (Figure 1). We first aimed to confirm that $O_3$ exposure leads to increased levels of GSSG. To this end we assessed the extent of intracellular glutathione oxidation in control and $O_3$-treated cells. We observed ≤ 3-fold increases in GSSG following 1 ppm $O_3$ exposure in LS – G as compared with air controls [see Supplemental Material, Figure S3 (http://dx.doi.org/10.1289/ehp.1206039)], which agrees with previous reports of the effect of $O_3$ exposure on intracellular glutathione (Chalfant and Bernd 2011; Todokoro et al. 2004).

Next, we asked whether the roGFP2 response to $O_3$ is influenced by glutaredoxin (Grx) activity. Grx is essential to mediate roGFP2 oxidation by GSSG (Figure 1), but Grx should play no role if roGFP2 is directly oxidized by $O_3$. On the one hand, we compared the response of roGFP2 (which interacts with endogenous Grx) with that of Grx1-roGFP2, a translational fusion of Grx1 and roGFP2. The fusion of these components is known to kinetically improve the equilibration between roGFP2 and GSSG in a highly specific manner (Gutscher et al. 2008; Meyer and Dick 2010). We found that the $O_3$-induced increase of $E_{GSH}$ in BEAS-2B cells expressing Grx1-roGFP2 occurred earlier and at a faster rate relative to that reported by cells expressing unlinked roGFP2, thus indicating
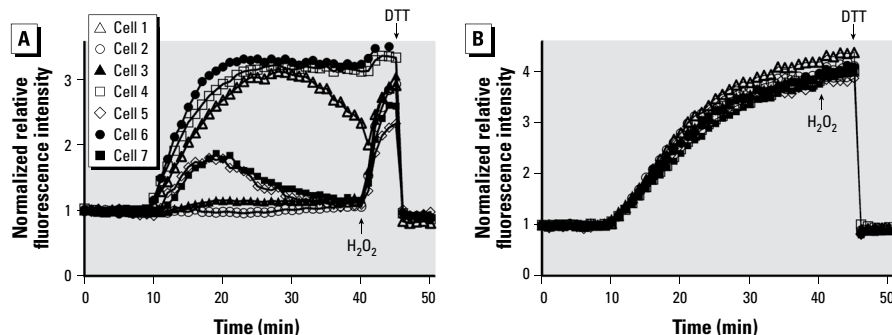


**Figure 3.** Glucose deprivation sensitizes cells to $O_3$-induced roGFP2 oxidation. Shown are the responses of seven BEAS-2B cells equilibrated in Locke solution containing 1 mg/mL glucose (LS + G: *A*), or 0 mg/mL (LS – G; *B*). Cells were exposed to 0.5 ppm $O_3$; addition of 0.1 mM $H_2O_2$ at the end of the $O_3$ exposure produced a maximal response, which was fully reversible with the addition of 10 mM DTT.

a GSSG/Grx–specific response (Figure 4A). In contrast, we investigated the effect of glutaredoxin inhibition by pretreating cells with the dithiocarbamate derivative 2-AAPA (Sadhu et al. 2012). The inhibitor completely blocked roGFP2 responses to O$_3$ and H$_2$O$_2$ (which also act indirectly through glutathione oxidation and reduction, respectively) (Figure 4B), thus confirming the role of Grx as the catalyst necessary for roGFP2 responsiveness to O$_3$. Together these observations confirm that O$_3$ is not simply sensed by the probe through direct oxidation, but rather by its specific effects on the glutathione redox couple.

Having confirmed that O$_3$ induces formation of GSSG, which is then detected by the roGFP2 probe, we asked whether glutathione peroxidases (GPx), major generators of GSSG, are involved in the O$_3$ response. Here we investigated the role of GPx activity in O$_3$-induced roGFP2 redox changes by pretreating BEAS-2B cells with 1 μM sodium selenite for ≤ 48 hr before O$_3$ exposure. Previous studies have used selenium supplementation as an effective means of increasing GPx expression, a finding that we also observed in preliminary studies with BEAS-2B cells [see Supplemental Material, Figure S4 (http://dx.doi.org/10.1289/ehp.1206039)] (Helmy et al. 2000; Holben and Smith 1999; Leist et al. 1996). Selenium-induced overexpression of GPx accelerated roGFP2 oxidation during a 0.5 ppm O$_3$ exposure (Figure 4C), suggesting that O$_3$ gives rise to peroxides, which are then converted by GPx to GSSG, which is in turn reported by roGFP2 through the intervention of Grx.

***Investigating the role of secondary products in O$_3$-induced redox changes.*** Because the data shown in Figure 4C suggested the involvement of peroxides in the O$_3$ response, we asked whether there is a specific role for H$_2$O$_2$. For these experiments we examined H$_2$O$_2$ generation as a consequence of O$_3$ exposure using the cytosolic-targeted H$_2$O$_2$ sensor, HyPer. O$_3$ caused a relatively modest increase in the HyPer response during the exposure period (Figure 5). However, the observed HyPer response did not precede nor match the magnitude of the roGFP2 response, making it unlikely that the observed increase in $E_{GSH}$ is primarily caused by H$_2$O$_2$ generation.

Mitochondrial oxidant production, frequently associated with increased oxidation of mitochondrial glutathione, has been implicated as a contributing factor in the cellular response to xenobiotics (Cheng et al. 2010, 2012; Hanson et al. 2004). Therefore, we next used mitochondrially targeted roGFP2 (roGFP2-mito) to assess the impact of O$_3$ exposure on the mitochondrial $E_{GSH}$ of BEAS-2B cells. As shown in Figure 6, exposure to 1 ppm O$_3$, twice the amount used for cytosolic assessments, induced an increase in mitochondrial $E_{GSH}$. However, relative to the cytosolic roGFP2 response, the increase in mitochondrial $E_{GSH}$ occurred at a slower rate and achieved a lower magnitude, suggesting that mitochondrial oxidants are not the primary source of the oxidants that lead to increased cytosolic $E_{GSH}$.

## Discussion

"Oxidative stress" is a frequently cited mechanistic component of the adverse health effects induced by numerous xenobiotic compounds (Bargagli et al. 2009; Chung and Marwick 2010; Ciencewicki et al. 2008; Jones 2008; Kohen and Nyska 2002; MacNee 2001; Ward 2010; Yang and Omaye 2009). However, the term "oxidative stress" is a very broad concept and the detection of early and specific indices of oxidant stress has proven to be methodologically difficult. The advent of genetically encoded fluorescent reporters that are sensitive to their redox environment has enabled real-time imaging-based assessments of oxidant outcomes in living cells with unprecedented spatial and temporal resolution. In this study, we validated the use of one such reporter, roGFP2, for the specific assessment of xenobiotic-induced changes in the $E_{GSH}$ using O$_3$ as a model toxicant and BEAS-2B cells as a model of the human bronchial epithelium.

The prooxidative change in $E_{GSH}$ observed in this study represents an early event in the oxidant injury caused by O$_3$. O$_3$ is a potent oxidant gas that has the potential to interact directly with virtually any cellular component, potentially including fluorescent reporter molecules such as roGFP2. Thus, in interpreting the probe response observed in O$_3$-exposed BEAS-2B cells, we had to consider the possibility that O$_3$ could be bypassing the glutathione system through which roGFP2 sensors normally respond (Gutscher et al. 2008; Meyer and Dick 2010).

Our findings strongly suggest that even in the presence of a strong oxidant like O$_3$, roGFP2 is oxidized only indirectly through its known coupling to the glutathione system. This conclusion is supported by several observations: First, glucose deprivation increased O$_3$-mediated roGFP2 oxidation, consistent with the requirement for NADPH in robustly maintaining $E_{GSH}$, the lack of glucose preventing regeneration of reducing equivalents throughout the exposure period. NADPH levels were approximately 70% lower in cells equilibrated in the absence of glucose, which appears to be sufficient to sensitize cells uniformly. In addition, it is important to bear in mind that other cellular processes also draw on the NADPH pool, and the continued lack of glucose largely prevents active regeneration of reducing equivalents throughout the exposure period.

Second, we confirmed the role of glutaredoxin in mediating the roGFP2 response to O$_3$. Grx1 is required to transfer oxidative equivalents from the glutathione pool to roGFP2. In previous studies using Grx1-roGFP2, the chimeric linkage of Grx1 to roGFP2 enhanced responses to physiological oxidants such as H$_2$O$_2$ (Gutscher et al. 2008; Meyer and Dick 2010). Importantly, Grx1-roGFP2 also accelerated the roGFP2
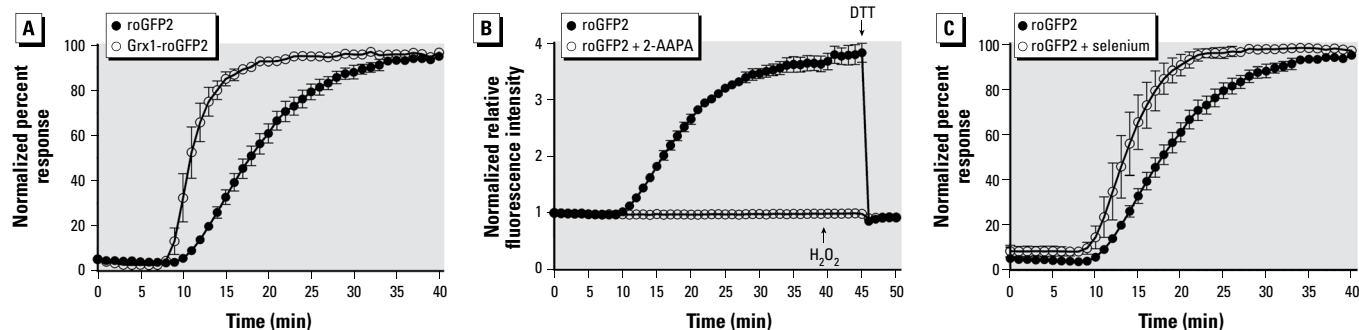


**Figure 4.** Manipulation of the glutathione system modulates roGFP2 responses to O$_3$. (*A*) Changes in cytosolic $E_{GSH}$ induced by 0.5 ppm O$_3$ exposure as reported by BEAS-2B cells expressing either roGFP2 or Grx1-roGFP2. (*B*) BEAS-2B cells were pretreated with 100 μM 2-AAPA, a glutaredoxin inhibitor, before exposure to 0.5 ppm O$_3$; the responses shown are the normalized 404/488 ratios plotted relative to their established baseline. (*C*) BEAS-2B cells were pretreated with 1 μM sodium selenite for 48 hr before 0.5 ppm O$_3$ exposure. To facilitate comparison of the responses in (*A*) and (*C*), the normalized ratios were plotted as a percentage of the signals obtained at maximal oxidizing and reducing conditions achieved using 1 mM H$_2$O$_2$ and 10 mM DTT, respectively. Other experimental conditions were as described for Figure 2. Values shown are mean ± SE ($n \geq 3$).

response to $O_3$, whereas inhibition of endogenous Grx with 2-AAPA prevented roGFP2 oxidation in the presence of $O_3$. Although early reports describe 2-AAPA as being an inhibitor of glutathione reductase, a more recent study reports that this dithiocarbamate derivative acts as a direct inhibitor of Grx as well (Sadhu et al. 2012). Thus, the finding that 2-AAPA–treated cells failed to respond to $O_3$ supports the involvement of Grx and is consistent with the claim that 2-AAPA is an inhibitor of Grx. Importantly, the fact that use of this inhibitor was effective at disconnecting the glutathione pool from the redox reporter argues against a nonspecific interaction between $O_3$, or a secondary oxidant, and the roGFP2 sensor.

Last, findings from experiments examining the effect of overexpression of glutathione peroxidases (GPx) using prolonged selenite supplementations are consistent with an upstream role of GPx in the oxidative pathway leading to $O_3$-induced roGFP2 oxidation. GPx couple the reduction of (hydro)peroxides to the generation of GSSG (Arthur 2000; Matés and Sánchez-Jiménez 1999; Meyer and Dick 2010). In our system, the increased expression of GPx-enhanced roGFP2 oxidation, suggesting that $O_3$ exposure generates (hydro)peroxides, which then drive the formation of GSSG. In fact, $O_3$ has been shown to produce many types of lipid hydroperoxides upon exposure (Mudway and Kelly 2000; Yang and Omaye 2009). Moreover, cells exposed to $O_3$ may have an increased $H_2O_2$ burden as well. Overall, the results from GPx-overexpressing cells suggest that the increased activity of these enzymes leads to an enhanced catalytic destruction of peroxides with concomitant GSH oxidation, leading to the roGFP2 response to $O_3$.

Using the $H_2O_2$ probe HyPer, our initial assessments suggested slightly elevated $H_2O_2$ production following $O_3$ exposure of BEAS-2B cells. The quantitative interpretation of HyPer responses is, however, difficult. It is not clear to what extent the OxyR domain of HyPer may be outcompeted by endogenous peroxidases. In addition, HyPer is highly pH sensitive, as much as the cpYFP module on which it is based (Schwarzländer et al. 2012). Thus, an $O_3$-induced intracellular acidification could dampen the HyPer response to $H_2O_2$. Nevertheless, following $O_3$ exposure, HyPer responded to exogenously applied $H_2O_2$ and DTT as expected, which demonstrates the general functionality of the probe. Taken together, the delayed time of onset, the slow rates of response, and the relatively low magnitude of the HyPer responses seem to suggest that $H_2O_2$ production is not a major factor in the total $O_3$-induced $E_{GSH}$ effects. Likewise, the measurements in mitochondrially targeted roGFP do not support a mitochondrial source for the $O_3$-induced increase in cytosolic $E_{GSH}$. These results suggest that the relevant oxidant species, potentially a hydroperoxide, is primarily generated in the cytosol or within the outer plasma membrane, and the mitochondrial $E_{GSH}$ response would be expected to lag behind that of the cytosol. Additionally, differences in peroxidase composition and activity may contribute to the lag in the $O_3$-induced mitochondrial $E_{GSH}$ response relative to the cytosol.

The studies presented herein cannot completely exclude a partial contribution of direct interactions between $O_3$, or its secondary by-products, with the thiols of the roGFP2 sensor. In addition, because the roGFP2 fluorescence ratio reflects $E_{GSH}$, which is a function of both the GSSG:GSH ratio and the total glutathione concentration, it is possible that $O_3$-induced electrophilic attack mediates the changes reported by roGFP2 by consuming reduced GSH. It should, however, be noted that the $E_{GSH}$ in the cytosol or mitochondrial matrix is much more sensitive to an increase in GSSG than to depletion of GSH. This is because the $E_{GSH}$ in the cytosol (around –320 mV, or even lower, in mitochondria) represents nanomolar GSSG in a millimolar pool of GSH. To deflect the roGFP2 signal from –320 mV to about –260 mV only requires the concentration of GSSG to increase from 200 nm to 20 μM (in a 10 mM total glutathione pool). To achieve the same magnitude of $E_{GSH}$ response by depleting GSH exclusively would require a loss of 90% of GSH (e.g., from 10 mM to 1 mM) (Meyer and Dick 2010). Such a massive depletion of GSH by parts-per-million concentrations of $O_3$ (which could generate only limited amounts of electrophiles) seems stochiometrically unlikely. If one also considers the relative kinetics of GSSG generation and consumption (GSSG generation by GPx exhibits second order rate constants in the range of $1 \times 10^8$ $M^{-1}$ $sec^{-1}$), it appears reasonable to suggest that the $O_3$ effect reported in our study is primarily due to GSSG generation and that the contribution of glutathionylated electrophile(s) formation is minor.

Thus, although several different $O_3$-induced processes may together drive glutathione oxidation, including lipid peroxidation, $H_2O_2$ generation, and other oxidizing processes, the available evidence strongly suggests that the cytosolic roGFP2 responses to $O_3$ exposure are appropriately reporting the $E_{GSH}$. Taken together, these results demonstrate that roGFP2-based sensors can be used to monitor shifts in glutathione redox homeostasis in $O_3$-exposed cells. Furthermore, the experimental approach we used may be utilized for the validation of "oxidant stress" induced by other reactive xenobiotics in living cells.

## Conclusion

Our results demonstrate the utility of using genetically encoded fluorescent reporters in making reliable assessments of cells undergoing exposure to xenobiotics with strong oxidizing properties.

**Figure 5.** Comparison between roGFP2 and HyPer responses to $O_3$. BEAS-2B cells expressing either roGFP2 or the $H_2O_2$ sensor, HyPer, were exposed to 0.5 ppm $O_3$ as described for Figure 2. To facilitate comparison, the normalized ratios were plotted as a percentage of the signals at maximal oxidation and reduction achieved using 1 mM $H_2O_2$ and 10 mM DTT, respectively. Values shown are mean ± SE ($n \geq 3$).

**Figure 6.** $O_3$-induced $E_{GSH}$ changes affect the cytosol more rapidly than the mitochondrial matrix. BEAS-2B cells expressing roGFP2 targeted to either the cytosol or mitochondria were exposed to either 0.5 ppm (roGFP2-cyto) or 1.0 ppm (roGFP2-mito). For direct comparison, the normalized ratios were plotted as a percentage of the maximal oxidation achieved using 1 mM $H_2O_2$ and 10 mM DTT. Other experimental conditions were as described in Figure 2. Values shown are mean ± SE ($n \geq 3$).

### References

Anderson ME. 1998. Glutathione: an overview of biosynthesis and modulation. Chem Biol Interact 111–112:1–14.

Arthur JR. 2000. The glutathione peroxidases. Cell Mol Life Sci 57:1825–1835.

Ballatori N, Krance SM, Notenboom S, Shi S, Tieu K, Hammond CL. 2009. Glutathione dysregulation and the etiology and progression of human diseases. Biol Chem 390:191–214.

Ballinger CA, Cueto R, Squadrito G, Coffin JF, Velsor LW, Pryor WA, et al. 2005. Antioxidant-mediated augmentation of ozone-induced membrane oxidation. Free Radic Biol Med 38:515–526.

Bargagli E, Olivieri C, Bennett D, Prasse A, Muller-Quernheim J, Rottoli P. 2009. Oxidative stress in the pathogenesis of diffuse lung diseases: a review. Respir Med 103:1245–1256.

Cannon MB, Remington SJ. 2008. Redox-sensitive green fluorescent protein: probes for dynamic intracellular redox responses. A review. Methods Mol Biol 476:51–65.

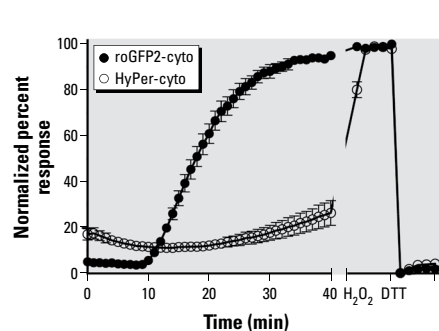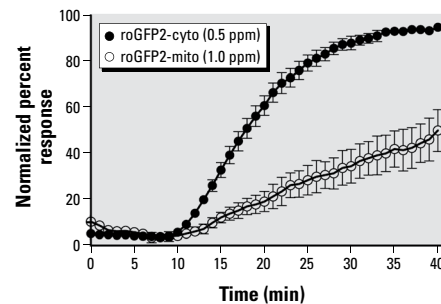Chalfant M, Bernd K. 2011. Detecting Ozone-Induced Changes in Cellular Redox Balance via GSH/GSSG-Glo™ Assay.

Available: http://www.promega.com/resources/ articles/pubhub/tpub_059-detecting-ozone-induced-changes-in-cellular-redox-balance-via-gsh-gssg-glo-assay/ [accessed 14 December 2012].

Cheng WY, Currier J, Bromberg PA, Silbajoris R, Simmons SO, Samet JM. 2012. Linking oxidative events to inflammatory and adaptive gene expression induced by exposure to an organic particulate matter component. Environ Health Perspect 120:267–274.

Cheng WY, Tong H, Miller EW, Chang CJ, Remington J, Zucker RM, et al. 2010. An integrated imaging approach to the study of oxidative stress generation by mitochondrial dysfunction in living cells. Environ Health Perspect 118:902–908.

Chung KF, Marwick JA. 2010. Molecular mechanisms of oxidative stress in airways and lungs with reference to asthma and chronic obstructive pulmonary disease. Ann NY Acad Sci 1203:85–91.

Ciencewicki J, Trivedi S, Kleeberger SR. 2008. Oxidants and the pathogenesis of lung diseases. J Allergy Clin Immunol 122:456–468.

Dooley CT, Dore TM, Hanson GT, Jackson WC, Remington SJ, Tsien RY. 2004. Imaging dynamic redox changes in mammalian cells with green fluorescent protein indicators. J Biol Chem 279:22284–22293.

Dubinina EE, Dadali VA. 2010. Role of 4-hydroxy-*trans*-2-nonenal in cell functions. Biochemistry (MOSC) 75:1069–1087.

Gutscher M, Pauleau AL, Marty L, Brach T, Wabnitz GH, Samstag Y, et al. 2008. Real-time imaging of the intracellular glutathione redox potential. Nat Methods 5:553–559.

Hanson GT, Aggeler R, Oglesbee D, Cannon M, Capaldi RA, Tsien RY, et al. 2004. Investigating mitochondrial redox potential with redox-sensitive green fluorescent protein indicators. J Biol Chem 279:13044–13053.

Helmy MH, Ismail SS, Fayed H, El-Bassiouni EA. 2000. Effect of selenium supplementation on the activities of glutathione metabolizing enzymes in human hepatoma Hep G2 cell line. Toxicology 144:57–61.

Holben DH, Smith AM. 1999. The diverse role of selenium within selenoproteins: a review. J Am Diet Assoc 99:836–843.

Jones DP. 2008. Radical-free biology of oxidative stress. Am J Physiol Cell Physiol 295:C849–C868.

Kelly FJ, Mudway I, Krishna MT, Holgate ST. 1995. The free radical basis of air pollution: focus on ozone. Respir Med 89:647–656.

Kohen R, Nyska A. 2002. Oxidation of biological systems: oxidative stress phenomena, antioxidants, redox reactions, and methods for their quantification. Toxicol Pathol 30:620–650.

Laumbach RJ. 2010. Outdoor air pollutants and patient health. Am Fam Physician 81:175–180.

Leist M, Raab B, Maurer S, Rösick U, Brigelius-Flohé R. 1996. Conventional cell culture media do not adequately supply cells with antioxidants and thus facilitate peroxide-induced genotoxicity. Free Radic Biol Med 21:297–306.

Ma Q. 2010. Transcriptional responses to oxidative stress: Pathological and toxicological implications. Pharmacol Ther 125:376–393.

MacNee W. 2001. Oxidative stress and lung inflammation in airways disease. Eur J Pharmacol 429:195–207.

Matés JM, Sánchez-Jiménez F. 1999. Antioxidant enzymes and their implications in pathophysiologic processes. Front Biosci 4:D339–D345.

Meyer AJ. 2008. The integration of glutathione homeostasis and redox signaling. J Plant Physiol 165:1390–1403.

Meyer AJ, Dick TP. 2010. Fluorescent protein-based redox probes. Antioxid Redox Signal 13:621–650.

Morgan B, Sobotta MC, Dick TP. 2011. Measuring $E_{GSH}$ and $H_2O_2$ with roGFP2-based redox probes. Free Radic Biol Med 51:1943–1951.

Mudway IS, Kelly FJ. 2000. Ozone and the lung: a sensitive issue. Mol Aspects Med 21:1–48.

Pryor WA. 1992. How far does ozone penetrate into the pulmonary air/tissue boundary before it reacts? Free Radic Biol Med 12:83–88.

Pryor WA, Squadrito GL, Friedman M. 1995. A new mechanism for the toxicity of ozone. Toxicol Lett 82–83:287–293.

Reddel RR, Ke Y, Gerwin BI, McMenamin MG, Lechner JF, Su RT, et al. 1988. Transformation of human bronchial epithelial cells by infection with SV40 or adenovirus-12 SV40 hybrid virus, or transfection via strontium phosphate coprecipitation with a plasmid containing SV40 early region genes. Cancer Res 48:1904–1909.

Sadhu SS, Callegari E, Zhao Y, Guan X, Seefeldt T. 2012. Evaluation of a dithiocarbamate derivative as an inhibitor of human glutaredoxin-1. J Enzyme Inhib Med Chem; doi:10.3109/14756366.2011.649267 [Online 3 February 2012].

Schwarzlander M, Murphy MP, Duchen MR, Logan DC, Fricker MD, Halestrap AP, et al. 2012. Mitochondrial 'flashes': a radical concept repHined. Trends Cell Biol 22:503-508.

Song H, Tan W, Zhang X. 2010. Ozone induces inflammation in bronchial epithelial cells. J Asthma 48:79–83.

Srebot V, Gianicolo EA, Rainaldi G, Trivella MG, Sicari R. 2009. Ozone and cardiovascular injury. Cardiovasc Ultrasound 7:30; doi:10.1186/1476-7120-7-30 [Online 24 June 2009].

Tal TL, Simmons SO, Silbajoris R, Dailey L, Cho S-H, Ramabhadran R, et al. 2010. Differential transcriptional regulation of IL-8 expression by human airway epithelial cells exposed to diesel exhaust particles. Toxicol Appl Pharmacol 243:46–54.

Taylor-Clark TE, Undem BJ. 2010. Ozone activates airway nerves via the selective stimulation of TRPA1 ion channels. J Physiol 588:423–433.

Todokoro M, Mochizuki H, Tokuyama K, Utsugi M, Dobashi K, Mori M, et al. 2004. Effect of ozone exposure on intracellular glutathione redox state in cultured human airway epithelial cells. Inflammation 28:105–114.

van der Vliet A, O'Neil CA, Eiserich JP, Cross CE. 1995. Oxidative damage to extracellular fluids by ozone and possible protective effects of thiols. Arch Biochem Biophys 321:43–50.

Wamelink M, Struys E, Jakobs C. 2008. The biochemistry, metabolism and inherited defects of the pentose phosphate pathway: a review. J Inherit Metab Dis 31:703–717.

Ward PA. 2010. Oxidative stress: acute and progressive lung injury. Ann NY Acad Sci 1203:53–59.

Yang W, Omaye ST. 2009. Air pollutants, oxidative stress and human health. Mutat Res 674:45–54.